

Spectroscopy of Hydrothermal Reactions 20: Experimental and DFT Computational Comparison of Decarboxylation of Dicarboxylic Acids Connected by Single, Double, and Triple Bonds

Jun Li and Thomas B. Brill*

Department of Chemistry and Biochemistry, University of Delaware, Newark, Delaware 19716

Received: February 26, 2002; In Final Form: July 3, 2002

The kinetics and pathways of decarboxylation of aqueous acetylenedicarboxylic acid at pH = 0.97–8.02 were studied in situ at 80–160 °C and 275 bar by using an FT-IR spectroscopy flow reactor with sapphire windows. The first-order (or pseudo first-order) rate constants and corresponding Arrhenius parameters were obtained for the neutral acid, monoanion, and dianion. The decarboxylation rates are in the order: $\text{HO}_2\text{CC}\equiv\text{CCO}_2^- > \text{HO}_2\text{CC}\equiv\text{CCO}_2\text{H} > ^-\text{O}_2\text{CC}\equiv\text{CCO}_2^-$. The decarboxylation mechanisms of these reactants and the propiolic acid product were analyzed by B3LYP/6-31+G(d) density functional theory. The transition state structures were found for the neutral acids and monoanions. In gas phase the transition state structure is a four-member ring involving C–C(O)–O–H. In aqueous solution a cyclic structure incorporating at least one water molecule forms. A comparison of transition state structures for the decarboxylation of β -saturated (succinic) and β -unsaturated (maleic, fumaric, and acetylenedicarboxylic) aliphatic diacids was made with and without incorporating a water molecule. Consistent with experiment, the calculated activation energy for H-atom transfer to the α carbon atom in the decarboxylation step follows the order $\text{C}\equiv\text{C} < \text{C}=\text{C} < \text{C}-\text{C}$.

Introduction

Decarboxylation is an important practical reaction of carboxylic acids in organic chemistry, biochemistry and geochemistry. Decarboxylation can proceed via heterolytic cleavage or homolytic cleavage of the C–C bond, although heterolytic cleavage is more common at hydrothermal conditions.¹ Heterolysis with the loss of CO₂ appears to occur by a variety of mechanisms which depend on the structure of the parent acid and the experimental conditions. The transition state structures for decarboxylation include: (1) nucleophilic bimolecular attack on the carbon atom of carboxylate group;¹ (2) formation of a cyclic structure involving hydrogen-bonding between H of the carboxylate group and an electronegative atom in the β position (e.g., oxygen^{2,3} or carbon^{4,5}); (3) proton shift in an α , β -unsaturated acid to form a β , γ -unsaturated acid⁶ followed by (2); and (4) proton shift to form a zwitterionic structure (e.g., 2-aminofornylacetic acids,^{2,7} orotic acid,⁸ or 4-pyridylacetic acid⁹). Low molecular mass carboxylic acids, such as formic and acetic acid, tend to have higher hydrothermal stability and require more reactive conditions for decomposition, such as wet oxidation,¹⁰ supercritical water oxidation,¹¹ and heterogeneous surface catalysis.^{11–14}

A study¹⁵ of the structure–reactivity of acetic acid derivatives revealed that both steric and electronic effects play a role in the decarboxylation rate, but the steric effect is more important in most cases. For example, the cyclic transition state structure^{2,3} as described by mechanism (2) above significantly reduces the energy barrier toward decarboxylation. The α -hydroxy acids, which lack this structure, have condition-dependent decomposition pathways^{16–19} involving competitive decarboxylation, dehydration, and decarboxylation.

Another class of carboxylic acids whose decarboxylation mechanisms are complicated are the unsaturated dicarboxylic

acids containing C=C and C≡C bonds in the backbone. For example, maleic acid and fumaric acid are difficult to decarboxylate at hydrothermal conditions. They decompose instead to simple acids such as formic, glyoxylic, and oxalic acids.²⁰ Decarboxylation occurs with oxidative conditions, such as in wet air oxidation²⁰ and electrooxidation.²¹ Another example of complex decarboxylation occurs with itaconic, citraconic, and mesaconic acids.^{5,22} Decarboxylation of citraconic acid and mesaconic acid occurs via the decarboxylation of itaconic acid, i.e., citraconic acid and mesaconic acid initially isomerize to itaconic acid, which then loses CO₂. Thus, the position of the C=C bond in the backbone influences the reaction rate and mechanism.

Among the saturated and unsaturated aliphatic diacids and monoacids, acetylenedicarboxylic and propiolic acids, which possess a C≡C bond in the backbone, were found to decarboxylate the fastest at hydrothermal conditions. The reason for this fact is addressed in this paper. In previous work Tommila and Kivinen²³ reported that acetylenedicarboxylic acid decomposed about 30% faster than its monoanion, but did not discuss the dianion. Hsu and Huang²⁴ determined the rate constant and Arrhenius parameters for decarboxylation of the neutral acid in acetophenone, and reported an unusually small preexponential factor.

The decarboxylation of carboxylic acids and derivatives containing the C≡C bond are well-suited for study with an FT-IR spectroscopy flow reactor using sapphire windows because both the C≡C bond and CO₂ intensely absorb in the available band-pass. The mechanisms of decarboxylation of acetylenedicarboxylic acid, its monoanion, and propiolic acid were analyzed by density functional theory. The transition state structures with and without water catalysis were found. The comparison of these transition state structures with those of other monoacids (formic, acetic, acrylic, and 3-butenic) and diacids (oxalic, malonic, maleic, fumaric, and succinic) was made to

* Corresponding author. E-mail: brill@udel.edu.

TABLE 1: Rate Constants and Arrhenius Parameters for Decarboxylation of Acetylenedicarboxylic Acid (k_0), Acetylenedicarboxylate Monoanion (k_1), and acetylenedicarboxylate dianion (k_2)

$T/^\circ\text{C}$	$k_0 \times 10^3/\text{s}^{-1}$	$k_1 \times 10^3/\text{s}^{-1}$	$k_2 \times 10^3/\text{s}^{-1}$
80	1.56 ± 0.62	3.86 ± 0.51	
90	5.86 ± 2.47	10.6 ± 2.5	
100	14.5 ± 4.6	29.7 ± 4.4	
110	38.1 ± 12.6	78.8 ± 13.4	
120	92.0 ± 26.0	207 ± 32.3	1.55 ± 0.11
130			3.93 ± 0.22
140			10.8 ± 0.3
150			21.7 ± 0.8
160			37.7 ± 1.8

	$k_0 \times 10^3/\text{s}^{-1}$	$k_1 \times 10^3/\text{s}^{-1}$	$k_2 \times 10^3/\text{s}^{-1}$
$E_a/\text{kJ mol}^{-1}$	115 ± 3.2 (126.36 ^a) (99.16 ^b)	115 ± 1.2 (125.52 ^a)	111 ± 8.6
$\ln(A, \text{s}^{-1})$	32.0 ± 1.1 (35.63 ^a) (9.90 ^b)	33.5 ± 0.4 (35.07 ^a)	27.6 ± 2.5
$\Delta S^\ddagger/\text{J K mol}^{-1} \text{ c}$	18.7	22.6	-24.8

^a Reference 23. ^b From ref 24 in acetophenone. ^c At 100 °C.

understand why the presence of the C≡C bond has such an acceleratory effect on the decarboxylation rate.

Experimental Section

Acetylenedicarboxylic acid (HO₂CC≡CCO₂H, 95%), monopotassium acetylenedicarboxylate (KO₂CC≡CCO₂H, 98%), maleic acid (*cis*-HO₂CCH=CHCO₂H, 99%), fumaric acid (*trans*-HO₂CCH=CHCO₂H, 99%), succinic acid (HO₂CCH₂-CH₂CO₂H, 99%), methacrylic acid (CH₃CH=CHCO₂H, 99%), and KOH were purchased from Aldrich Chemical Co. and used without further purification. Milli-Q deionized water was sparged with compressed Ar before use to expel the atmospheric gases. The solution of dipotassium acetylenedicarboxylate was prepared by titrating an acetylenedicarboxylic acid solution with KOH to the equivalent point. The other solutions with different pH values (Table 2) were prepared by dissolving the diacid and monopotassium salt in the required ratios. For example, the solution with pH = 2.17 was prepared by mixing KO₂CC≡CCO₂H and HO₂CC≡CCO₂H in the ratio of 4:1 at 25 °C. The pH values of the solutions were measured at room temperature with an Orion model 330 pH meter. The concentrations of all solutions were 0.25 molal.

The flow reactor-IR spectroscopy cell constructed from titanium with sapphire windows and gold foil seals has been described in detail elsewhere.^{25,26} The temperature and pressure were controlled within ± 1 °C and ± 1 bar, respectively. The chosen flow rate in the 0.1–1.0 mL/min range was controlled with an accuracy of 1% by the use of an Isco syringe pump. Correction of the flow rate was made to account for the density change with temperature. Transmission IR spectra were recorded at 4 cm⁻¹ resolution with a Nicolet 560 Magna FTIR spectrometer and an MCT-A detector. Background spectra recorded on pure water at the same conditions were subtracted. Thirty-two spectra were summed at each condition and the rate data reported herein are the average of three replicated measurements.

During the decarboxylation reaction, the asymmetric stretches of aqueous CO₂ centered at 2343 cm⁻¹ and the C≡C triple bond at 2113 cm⁻¹ for propiolic acid and 2090 cm⁻¹ for the propiolate anion were observed in the band-pass of sapphire. To obtain the kinetic parameters, the band area of CO₂ was converted into concentration at each condition by using the Beer–Lambert Law and the previously determined molar absorptivity of aqueous

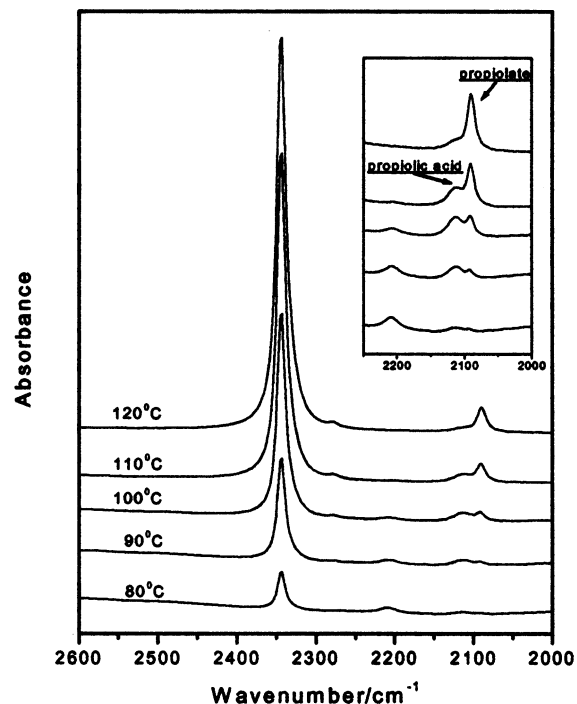


Figure 1. FT-IR spectra of 0.25 *m* monopotassium acetylenedicarboxylate at 275 bar and a residence time of 47 s as a function of temperature.

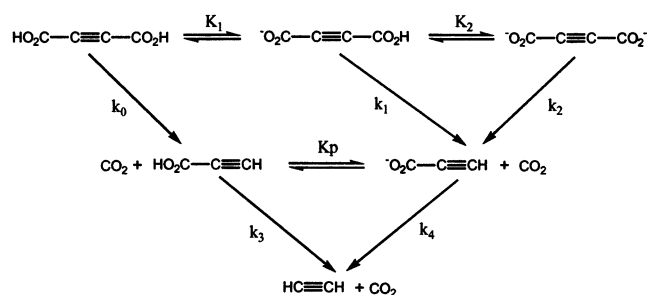
CO₂.²⁷ The molar absorptivities of the 2113 cm⁻¹ band and 2090 cm⁻¹ band were determined to be 4.5 times and 9 times smaller than that of CO₂, respectively. The concentrations of propiolic acid and propiolate anion were obtained by fitting the band area of 2113 and 2090 cm⁻¹ with a four-parameter Voigt function. Weighted least-squares regression²⁸ with a 95% confidence interval was performed for both the rate constants and the Arrhenius parameters in which the statistical weight was set to be $1/\sigma^2$, where σ is the standard deviation of the variables. Succinic, maleic, fumaric, and methacrylic acids did not decompose even when the flow reactor was run at its limit (330 °C and 275 bar) with a residence time of 60 s.

The density functional theory calculations on the transition state structures for decarboxylation were performed using Gaussian 98 software²⁹ at the level of theory of B3LYP^{30,31} with the basis set of 6-31G and 6-31+G(d). The geometries of reactants and transition state structures were optimized and vibrational frequency analyses were conducted to confirm that the optimized geometry was a local minimum or a transition state. The frequency analyses also provide thermal energy corrections to the total energy. All calculations were made at 298.15 K and 1 bar. The effect of temperature and pressure changes on the calculation was found to be negligible relative to the uncertainty in the computational method. In any event the comparisons made herein are best viewed as relative rather than absolute.

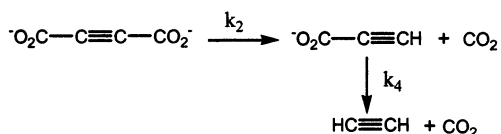
Kinetics

Reaction Pathways. Acetylenedicarboxylic acid decarboxylates to produce CO₂ and propiolic acid. Simultaneously, propiolic acid decarboxylates to form CO₂ and acetylene. In hydrothermal solutions, these reaction pathways were clearly indicated in situ using FT-IR spectroscopy and confirmed by comparing the spectra with those of the pure compounds. Real-time FT-IR spectra during the decarboxylation of 0.25 *m* monopotassium acetylenedicarboxylate are shown in Figure 1

SCHEME 1



SCHEME 2



at different temperatures with a pressure of 275 bar and a residence time of about 47 s. The existence of aqueous phase CO_2 (2343 cm^{-1}), propiolic acid (2113 cm^{-1}), and propiolate anion (2090 cm^{-1}) is clearly indicated. Two additional weak peaks were not identified.

Scheme 1 summarizes the reaction pathway in which K_1 , K_2 , and K_p are the first and second dissociation constants of acetylenedicarboxylic acid and the dissociation constant of propiolic acid, respectively; k_0 , k_1 , and k_2 are the rate constants of the neutral diacid, monoanion, and dianion of acetylenedicarboxylic acid; and k_3 and k_4 are the rate constants of propiolic acid and the propiolate anion, respectively. Acetylenedicarboxylic acid ($\text{p}K_1 = 1.23$ and $\text{p}K_2 = 2.53$) and propiolic acid ($\text{p}K_p = 1.89$) are rather strong acids which are mostly dissociated into the corresponding anions. Therefore, before and during decarboxylation, the dissociation equilibration of acetylenedicarboxylic acid and propiolic acid must be taken into account, and CO_2 potentially forms from all of the acetylenedicarboxylic acid and propiolic acid species.

Reaction Rates. The dissociation constants needed for calculation of the species distribution at high temperatures were extrapolated from room temperature³² by using the iso-Coulombic method³³ employing the specific volume³⁴ and ionization constants³⁵ of water. The prepared dipotassium acetylenedicarboxylate solution contains only 0.05% of the monoanion and 0.0004% of the diacid at $100\text{ }^\circ\text{C}$. It is difficult to obtain analytic rate expressions for all species because of the multiple reaction pathways shown in Scheme 1, but the analytic rate expressions can be derived when the acetylenedicarboxylate dianion predominates and Scheme 2 applies. The rate expressions 1–3 are appropriate when calculating k_2 , where C_{A0} is the initial concentration of $\text{}^-\text{O}_2\text{C}\equiv\text{C}\equiv\text{CO}_2^-$, C_B is the concentration of $\text{HC}\equiv\text{CCO}_2^-$, C_C is the total concentration of CO_2 in aqueous solution, i.e., eq 4, and k_4 is our previously determined rate constant for the propiolate anion.³⁶ C_C ,

$$C_A = C_{A0}e^{-k_2t} \quad (1)$$

$$C_B = \frac{C_{A0}k_2}{k_4 - k_2}(e^{-k_2t} - e^{-k_4t}) \quad (2)$$

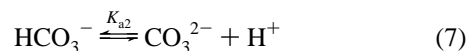
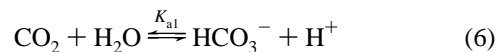
$$C_C = 2C_{A0} - \frac{C_{A0}}{k_4 - k_2}[(2k_4 - k_2)e^{-k_2t} - k_2e^{-k_4t}] \quad (3)$$

which is given by eq 4, was calculated by eq 5, which describes

the hydrolysis of CO_2 in basic solution. Equation 5 was parametrized by the use of eqs 6 and 7.³⁷

$$C_C = [\text{CO}_2]_{\text{obs}} + [\text{HCO}_3^-] + [\text{CO}_3^{2-}] \quad (4)$$

$$= [\text{CO}_2]_{\text{obs}} \left(1 + \frac{K_{a1}}{[\text{H}^+]} + \frac{K_{a1}K_{a2}}{[\text{H}^+]^2} \right) \quad (5)$$



This procedure enables the rate constant k_2 for $\text{}^-\text{O}_2\text{C}\equiv\text{C}\equiv\text{CO}_2^-$ to be obtained by fitting eq 2. The calculated values of the rate constant k_2 are given in Table 1 at $\text{pH} = 8.02$.

The determination of the rate constants for $\text{HO}_2\text{C}\equiv\text{C}\equiv\text{CO}_2\text{H}$ and $\text{HO}_2\text{C}\equiv\text{C}\equiv\text{CO}_2^-$ is different from that of $\text{}^-\text{O}_2\text{C}\equiv\text{C}\equiv\text{CO}_2^-$. From experiment,³⁸ propiolic acid and propiolate anion were observed to require higher temperatures to obtain the same decarboxylation rate as the acetylenedicarboxylic acid species. Hence, at lower temperatures in the early stage of decarboxylation, the CO_2 from the propiolic acid species is very small and can be ignored. The rate of formation of CO_2 follows eq 8 assuming that the first-order rate law applies to the decomposition of acetylenedicarboxylic acid species.

$$v = k_{\text{obs}}[\text{HO}_2\text{C}\equiv\text{C}\equiv\text{CO}_2\text{H}]_{T,t} \quad (8)$$

The observed first-order rate constant is k_{obs} , and the total acetylenedicarboxylic acid concentration as a function of time is given by eq 9.

$$\begin{aligned}
 [\text{HO}_2\text{C}\equiv\text{C}\equiv\text{CO}_2\text{H}]_{T,t} &= [\text{HO}_2\text{C}\equiv\text{C}\equiv\text{CO}_2\text{H}]_t + \\
 &[\text{HO}_2\text{C}\equiv\text{C}\equiv\text{CO}_2^-]_t + [\text{}^-\text{O}_2\text{C}\equiv\text{C}\equiv\text{CO}_2^-]_t = \\
 &[\text{HO}_2\text{C}\equiv\text{C}\equiv\text{CO}_2\text{H}]_0 - [\text{CO}_2]_{T,t} \quad (9)
 \end{aligned}$$

$[\text{HO}_2\text{C}\equiv\text{C}\equiv\text{CO}_2\text{H}]_0$ is the initial concentration of acetylenedicarboxylic acid. The calculation of the total concentration of CO_2 (eq 5) requires that the solution pH be known at each temperature and residence time during decarboxylation. At low pH, the hydrolysis of CO_2 to HCO_3^- and CO_3^{2-} is entirely negligible. In fact, except for $\text{KO}_2\text{C}\equiv\text{C}\equiv\text{CO}_2\text{K}$ at $\text{pH} = 8.02$, all of the experiments were conducted in this pH range starting from a solution pH of 0.97 (the natural pH of acetylenedicarboxylic acid) to the upper limit of 2.17. That the observed rate constants were first-order was confirmed as illustrated by the rate plot in Figure 2 for decarboxylation of $0.25\text{ m KO}_2\text{C}\equiv\text{C}\equiv\text{CO}_2\text{H}$. The observed first-order rate constants at different pH values in the range of 0.97–2.17 are listed in Table 2.

When the decarboxylation of $\text{HO}_2\text{C}\equiv\text{C}\equiv\text{CO}_2\text{H}$, $\text{HO}_2\text{C}\equiv\text{C}\equiv\text{CO}_2^-$, and $\text{}^-\text{O}_2\text{C}\equiv\text{C}\equiv\text{CO}_2^-$ follow first-order, eqs 10 and 11 apply.

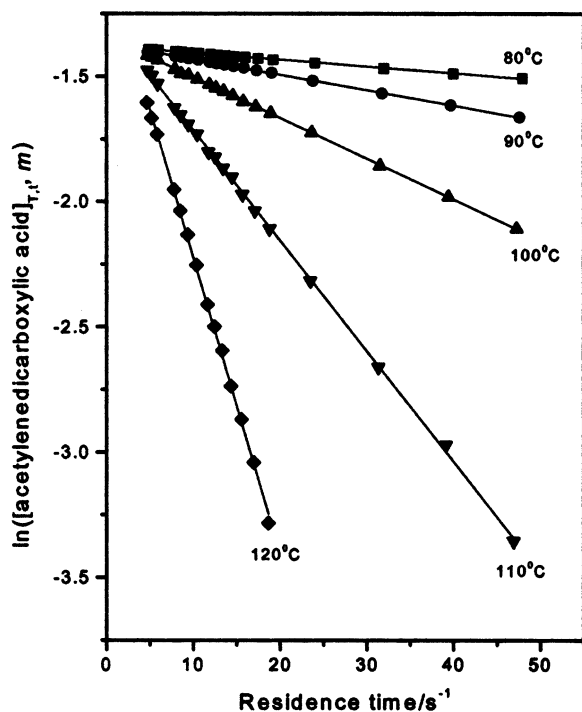
$$v = k_0[\text{HO}_2\text{C}\equiv\text{C}\equiv\text{CO}_2\text{H}]_t + k_1[\text{HO}_2\text{C}\equiv\text{C}\equiv\text{CO}_2^-]_t + k_2[\text{}^-\text{O}_2\text{C}\equiv\text{C}\equiv\text{CO}_2^-]_t \quad (10)$$

$$k_{\text{obs}} = \frac{k_0[\text{H}^+]^2 + k_1[\text{H}^+]K_1 + k_2K_1K_2}{[\text{H}^+]^2 + [\text{H}^+]K_1 + K_1K_2} \quad (11)$$

Fitting of the nonlinear eq 11 with the observed rate constants, ionization constants K_1 and K_2 , the rate constant k_2 , and solution pH at high-temperature yields rate constant k_0 for $\text{HO}_2\text{C}\equiv\text{C}\equiv\text{CO}_2\text{H}$

TABLE 2: Observed First-Order Rate Constants ($k_{\text{obs}} \times 10^3/\text{s}^{-1}$) for Decarboxylation of 0.25 *m* Acetylenedicarboxylic Acid at Different pH Values

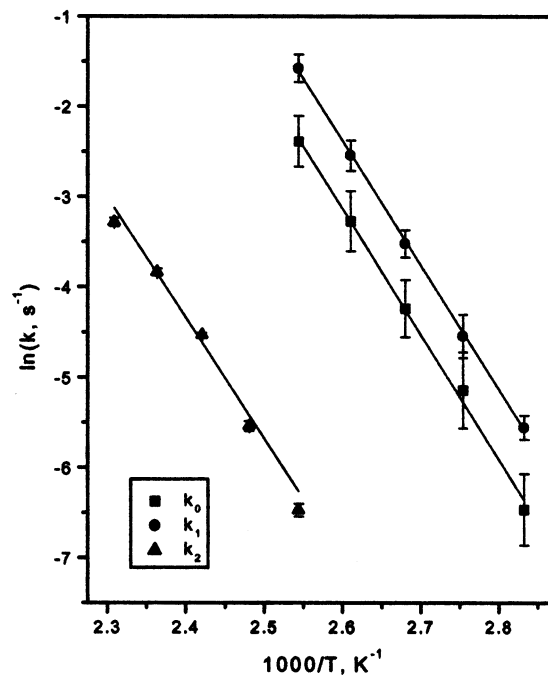
$T/^\circ\text{C}$	pH_{25}					
	0.97	1.36	1.52	1.66	1.91	2.17
80	1.43 ± 0.022	2.90 ± 0.05	2.53 ± 0.04	2.60 ± 0.05	2.70 ± 0.02	1.83 ± 0.02
90	4.36 ± 0.04	9.38 ± 0.14	7.28 ± 0.08	6.84 ± 0.06	6.19 ± 0.03	5.24 ± 0.05
100	14.2 ± 0.2	18.9 ± 0.3	23.1 ± 0.4	23.2 ± 0.3	16.3 ± 0.1	13.9 ± 0.4
110	36.9 ± 0.5	47.6 ± 0.4	61.5 ± 1.0	59.4 ± 0.7	44.1 ± 0.2	33.0 ± 0.8
120	97.6 ± 2.7	110.1 ± 1.1	153.7 ± 2.8	143.9 ± 3.5	123.4 ± 2.0	61.6 ± 1.2

**Figure 2.** Rate plot for the decarboxylation of 0.25 *m* monopotassium acetylenedicarboxylate at different temperatures and 275 bar.

CCO_2H and k_1 for $\text{HO}_2\text{CC}\equiv\text{CCO}_2\text{H}$. The solution pH at high temperatures can be calculated fortunately from the concentration ratio of propiolic acid and propiolate anion (eq 12).

$$[\text{H}^+] = K_p[\text{HC}\equiv\text{CCO}_2\text{H}]/[\text{HC}\equiv\text{CCO}_2^-] \quad (12)$$

The pH values obtained are a little higher than the initial solution pH values calculated from the charge balance equation at high temperatures. This is not surprising because the reactant acetylenedicarboxylic acid and the product propiolic acid are relatively strong acids and the decomposition yields are not high. In fact, the pH at the mean value of the different residence times was used to represent the real solution pH at a given temperature. The obtained rate constants k_0 and k_1 and Arrhenius parameters are given in Table 1. The Arrhenius plots are displayed in Figure 3. Clearly, the decarboxylation rates of acetylenedicarboxylic acid species are in the order: $\text{HO}_2\text{CC}\equiv\text{CCO}_2^- > \text{HO}_2\text{CC}\equiv\text{CCO}_2\text{H} > ^-\text{O}_2\text{CC}\equiv\text{CCO}_2^-$. For comparison, the previously reported activation energies and preexponential factors of neutral acid and monoanion in aqueous solution, as well as that of neutral acid in acetophenone are also listed in Table 1. The Arrhenius parameters determined by Tommila and Kivinen²¹ are close to those of this work, but the preexponential factor for the neutral acid in acetophenone reported by Hsu and Huang²² is probably too small even when the effect of the solvent is taken into account. The decarboxylation rate of the dianion is the slowest, which is also the case with malonic acid.³⁹ The same order of rates is expected for oxalic acid⁴⁰ and

**Figure 3.** Arrhenius plot for the decarboxylation of neutral acetylenedicarboxylic acid, acetylenedicarboxylate monoanion, and acetylenedicarboxylate dianion.

phenylmalonic acid⁴¹ when the rate constants for the dianions are inferred from those of the acid as a function of the pH.

Mechanisms by Density Functional Theory

Geometries and Energetics. The optimized geometries and energetics of the neutral acids and their anions are shown in Figure 4 (ACDC represents $\text{HO}_2\text{CC}\equiv\text{CCO}_2\text{H}$, ACDC^- is $\text{HO}_2\text{CC}\equiv\text{CCO}_2^-$, and Prop is $\text{HC}\equiv\text{CCO}_2\text{H}$). From Figure 4 it can be seen that the conformers in which the hydrogen atom is anti to the carbonyl oxygen (hereinafter the anti carboxylic hydrogen) are higher in energy than the syn conformers. Nagy⁴² also observed this pattern. The C–C single bond lengths adjacent to the $\text{C}\equiv\text{C}$ triple bond are about 0.07 Å shorter than that of a normal C–C bond (ca. 1.51 Å) as a result of resonance of the lone pair atomic orbitals on the oxygen atoms with the $\text{C}\equiv\text{C}$ bond. This significant delocalization of excess negative charge for acetylenedicarboxylate anion was evident to Skurski et al.,⁴³ when the acetylenedicarboxylate and succinate dianions were compared, and was proposed to be the reason for why succinate anion was not easily observed by photoelectron spectroscopy. Another finding in the calculations of Figure 4 is that the carbon chain backbone increases in length by 0.04 Å and 0.07 Å, respectively, when the neutral acid dissociates into the monoanion and the dianion. Dissociation produces negative charge on the terminal carboxylate groups, and the resulting electrostatic repulsion stretches the carbon chain and forces the dihedral angle of the two carboxylate groups to approach 90°.

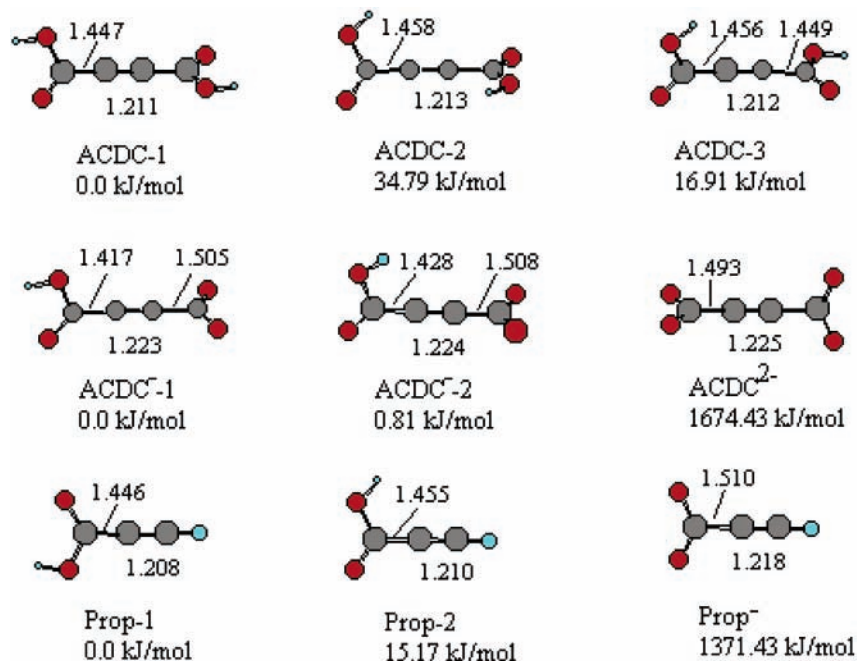


Figure 4. Geometries and relative energetics of acetylenedicarboxylic acid and propiolic acid species at the level of B3LYP/6-31+G(d). The bond lengths are given in angstroms.

Transition State Structures. The global decarboxylation reaction of aliphatic acids is given by eq 13:



The proton-transfer step is a key element of the decarboxylation process. Ab initio and DFT calculations have been carried out for the decarboxylation process of many acids including formic,^{44–48} acetic,^{49–52} 3-butenic,⁴ acrylic,⁵³ oxalic,^{54,55} malonic,^{2,3} and itaconic.⁵ Among the transition state structures obtained, the six-member ring in malonic acid (involving intramolecular hydrogen bonding),^{2,3} 3-butenic acid,⁴ and itaconic acid⁵ leads to proton transfer as a low energy barrier process. The similar transition state consisting of a six-member ring structure is impossible for acetylenedicarboxylic and propiolic acid, because the C≡C bond forces linearity. Hence the transition state structure in which the carboxylate hydrogen atom starts in the anti orientation and forms a four-member ring structure is the only reasonable structure, but has a high energy barrier because of the strain energy. However, when one water molecule participates to form a six-member ring structure, the energy barrier is significantly reduced. The involvement of two water molecules reduces the energy even more,^{44,48,49,53,56} but the incremental difference is smaller than that produced by the first water molecule. The resulting transition states with and without participation of one water molecule are shown in Figure 5. The energy barrier for decarboxylation of HO₂CC≡CCO₂H is 118.7 kJ/mol when one water molecule acts as a catalyst, which is in excellent agreement with the experimental value of 115.5 kJ/mol in Table 1. For HO₂CC≡CCO₂⁻, the calculated value of 66.6 kJ/mol is about half the experimental value of 114.6 kJ/mol, and the value for HC≡CCO₂H of 124.7 kJ/mol is larger than the experimental value of 88 kJ/mol.³⁸ The origin of the differences for the latter two compounds is discussed further below.

It should be pointed out that the reference state for the calculation of the energy barrier is that in which the reactant molecule and water molecule are separated at infinite distance. When solvation by one water molecule was considered, the

energy barriers increased because of the additional energy of the hydrogen bonds between reactant and the water molecule. We compared the energy barrier of the transition state with water present but without participation of water in the proton transfer step. Four water molecules were positioned to interact with the external regions of the carboxylate groups. The results are shown in Figure 6. There was no difference in energy barrier for the intramolecular proton transfer process when 1, 2, 3, or 4 water molecules surrounded the reactant in this manner. A similar result has recently been obtained for carbonic acid.⁵⁶ The effect of more extensive solvation on the energy barrier was not considered because there are many possible orientations of water molecules when surrounding the reactant. However, a conclusion that may be drawn from these calculations, as well as those for carbonic acid, is that small changes in solvent density do not affect the transition state.

The difference in the calculated and experimental activation energy for HO₂CC≡CCO₂⁻ may arise from at least three factors: The choice of the reference state; the fact that no counteraction was incorporated; and the fact that no solvation shell was included in the calculation. Also, the experimental value of E_a for HC≡CCO₂H may have been affected by slight curvature in the rate plots³⁸ making the value somewhat uncertain.

Another finding is that the dihedral angle of the two carboxylate groups is close to 0° when one water molecule is incorporated into neutral acetylenedicarboxylic acid and its monoanion (see Figure 5), whereas the angle is 90° in the unsolvated structure. However, this angle is retained at about 90° when solvation of the solute by up to four water molecules occurs and two water molecules coordinate each carboxylate group to form a hydrogen bond net (Figure 6). This is an extreme example showing that solvation differences can cause a conformational change.

Why Do Acetylenedicarboxylic and Propiolic Acids Decarboxylate So Easily? Acetylenedicarboxylic and propiolic acids decarboxylate readily at 80–160 °C. On the other hand, there is no evidence of decarboxylation of succinic, maleic, fumaric, and methacrylic acids when the flow reactor was run

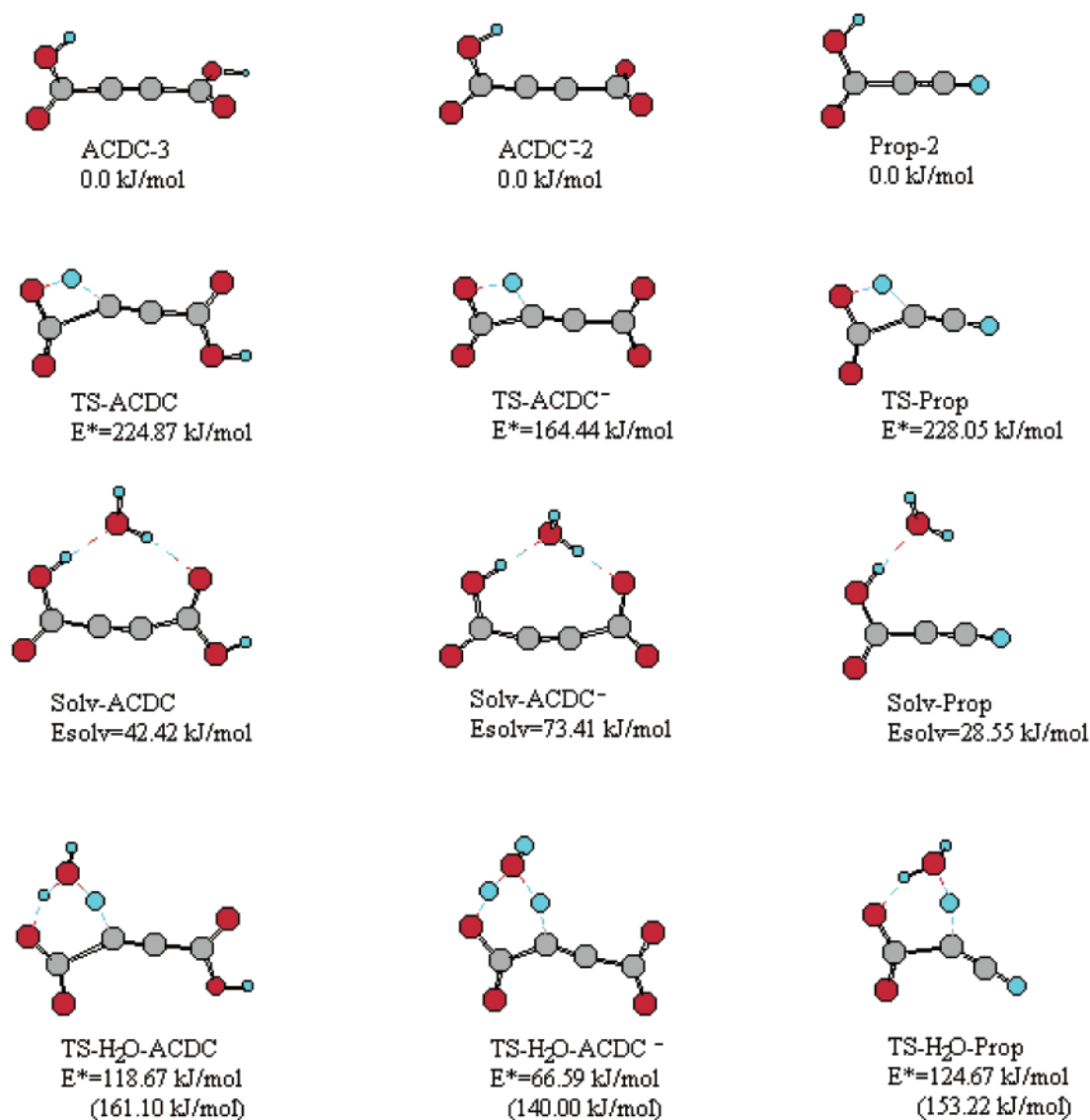


Figure 5. Transition state structures leading to decarboxylation with and without the participation of one water molecule and the starting structures for $\text{HO}_2\text{CC}\equiv\text{CCO}_2\text{H}$, $\text{HO}_2\text{CC}\equiv\text{CCO}_2^-$, and $\text{HC}\equiv\text{CCO}_2\text{H}$ at the level of B3LYP/6-31+G(d). The values in parentheses are the activation energies calculated starting from the solvated structures.

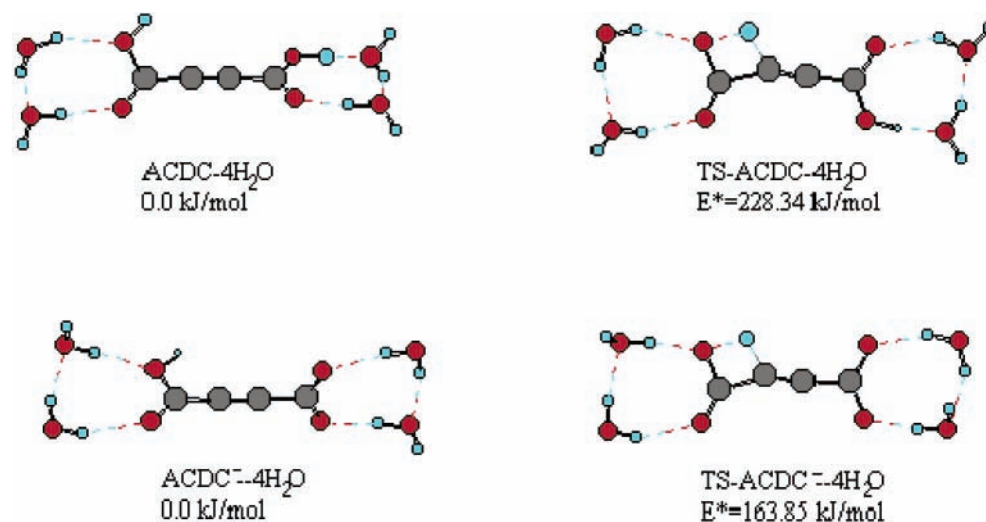


Figure 6. The effect of solvation of the carboxylate groups on the energy barrier of decarboxylation for $\text{HO}_2\text{CC}\equiv\text{CCO}_2\text{H}$ and $\text{HO}_2\text{CC}\equiv\text{CCO}_2^-$.

at its limit (330 °C and 275 bar) for 60 s. As discussed above, the six-member cyclic structure with the carboxylate hydrogen atom transferring to the β -position oxygen atom^{2,3} is energeti-

cally the lowest pathway for malonic acid. When such a structure was applied to maleic^{57,58} acid and itaconic acid ($=\text{CH}_2$ in the β -position),⁵⁹ decarboxylation did not occur. Instead, the transi-

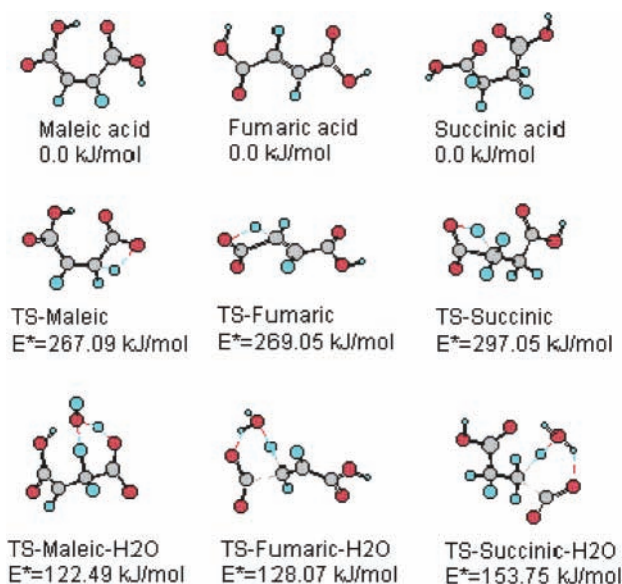


Figure 7. Transition state structures at the level of B3LYP/6-31G for decarboxylation with and without the participation of one water molecule and the starting structures of maleic, fumaric, and succinic acids.

tion state structures found corresponded to that for a low barrier hydrogen bond,^{60,61} in which the distance between two hydrogen atom acceptors is short enough to reduce the energy barrier for H transfer.

Alternatively, proton transfer leading to the release of CO₂ can occur via a four-member ring structure starting from the anti carboxylic hydrogen conformer. The energy barriers for this process in formic,^{44–48} acetic,⁵² oxalic,⁵⁴ malonic,³ 3-oxopropanoic,³ and acetoacetic³ acids are in the vicinity of 290 kJ/mol (except for 3-oxopropanoic acid which is 375.7 kJ/mol), which are much higher than those for acetylenedicarboxylic and propiolic acids. This is the case irrespective of the use of different theories and basis sets (e.g., HF, MP2, MP4, B3LYP, 6-31G, and 6-311G(d)) for these acids. For further clarification, the transition state structures were calculated at the level of B3LYP/6-31G for maleic (β -cis C=C), fumaric (β -trans C=C), and succinic (C–C) acids and are displayed in Figure 7. The conformational analyses of maleic,⁶² fumaric,⁶² and succinic⁶³ acids have been performed previously resulting in five conformations for maleic and fumaric acids, and fifteen conformations for succinic acid. Two anti conformations not previously found⁶² were found in the present study. One of the anti conformers was chosen here for each acid to conduct detailed calculations. These calculations reveal the probable reason for the decarboxylation rate differences. Compared to the ease of the carboxylic hydrogen atom transferring to the carbon atom of C–C bond, there is a reduction of 30 kJ/mol in the energy barrier when this hydrogen atom transfers to the carbon atom of C=C bond, and a reduction of 73 kJ/mol when this hydrogen atom transfers to the carbon atom of C≡C bond. Therefore, if the hydrogen atom acceptor is a C≡C bond, the energy barrier to proton transfer is the smallest, with or without participation of water molecules. The inclusion of one water molecule in the transition state structure reduces energy barrier to about half that without the water molecule. Succinic acid with and without water molecules has the highest calculated activation energy among the diacids. The energy barriers toward decarboxylation of maleic and fumaric acids (Figure 7) are higher than those needed for isomerization (66 kJ/mol),⁶⁴ hydration (94 kJ/mol),⁶⁵ or decomposition to simple acids (56.6 kJ/mol for maleic and 71 kJ/mol for fumaric).²⁰

Conclusions

The decarboxylation rates of acetylenedicarboxylic species follow the order: HO₂CC≡CCO₂[−] > HO₂CC≡CCO₂H > [−]O₂CC≡CCO₂[−]. The experimentally determined activation energies for these three species are approximately 113 kJ/mol. The transition state structures were found for the reactant acid species (neutral acid and monoanion) and product acid species (propiolic acid) by using density function theory at the level of B3LYP/6-31+G(d). In gas phase, the transition state structure is a four-member ring involving C–C(O)–OH with the proton transferring from the carboxylate group to the α -carbon. In aqueous solution, a cyclic structure incorporating at least one water molecule forms. The difference in the calculated activation energies for HO₂CC≡CCO₂H and HC≡CCO₂H is consistent with their relative hydrothermal reactivity based on the experimental data.

A comparison of the calculated activation energy for the decarboxylation of β -saturated and β -unsaturated aliphatic diacids revealed that the order is C–C > C=C > C≡C. Incorporation one water molecule in the transition state structure reduced the energy barrier to about half that without the water molecule, but did not change the ordering. The same order for decarboxylation rate is found in the experimental data.

Acknowledgment. We are grateful to the National Science Foundation for support of this work on Grant CHE-9807370.

References and Notes

- Clark, C. L. In *The Chemistry of Carboxylic Acids and Esters. The Chemistry of Functional Groups*; Patai, S., Ed.; Wiley: New York, 1969; p 589.
- Bach, R. D.; Canapa, C. J. *Org. Chem.* **1996**, *61*, 6346.
- Huang, C. L.; Wu, C., C.; Lien, M. H. *J. Phys. Chem. A* **1997**, *101*, 7867.
- Wang, Y. L.; Poirier, R. A. *Can. J. Chem.* **1994**, *72*, 1338.
- Li, J.; Brill, T. B. *J. Phys. Chem. A* **2001**, *105*, 10839.
- Arnold, R. T.; Elmer, O. C.; Dodson, R. M. *J. Am. Chem. Soc.* **1950**, *72*, 4350.
- Bach, R. D.; Canapa, C. J. *Am. Chem. Soc.* **1997**, *119*, 11725.
- Phillips, L. M.; Lee, J. K. *J. Am. Chem. Soc.* **2001**, *123*, 12067.
- Sicinska, D.; Truhlar, D. G.; Paneth, P. J. *Am. Chem. Soc.* **2001**, *123*, 7683.
- Shende, R. V.; Levec, J. *Ind. Eng. Chem. Res.* **1999**, *38*, 3830.
- Yu, J. L.; Savage, P. E. *Ind. Eng. Chem. Res.* **1998**, *37*, 2.
- Maiella, P. G.; Brill, T. B. *J. Phys. Chem. A* **1998**, *102*, 5886.
- Palmer, D. A.; Drummond, S. E. *Geochim. Cosmochim. Acta* **1986**, *50*, 813.
- Bell, J. L. S.; Palmer, D. A. *Organic Acids in Geological Processes*; Springer-Verlag: Berlin, 1994; p 227.
- Belsky, A. J.; Maiella, P. G.; Brill, T. B. *J. Phys. Chem. A* **1999**, *103*, 4253.
- Domingo, L. R.; Andres, J.; Moliner, V.; Safont, V. S. *J. Am. Chem. Soc.* **1997**, *119*, 6415.
- Li, L. X.; Portela, J. R.; Vallejo, D.; Gloyna, E. T. *Ind. Eng. Chem. Res.* **1999**, *38*, 2599.
- Mok, W. S.-L.; Antal, M. J. *J. Org. Chem.* **1989**, *54*, 4596.
- Lira, C. T.; McCrackin, P. J. *Ind. Eng. Chem. Res.* **1993**, *32*, 2608.
- Shende, R. V.; Levec, J. *Ind. Eng. Chem. Res.* **2000**, *39*, 40.
- Cataldo F.; Progega, S. N. C. *Croat. Chem. Acta* **2000**, *73*, 435.
- Carlsson, M.; Habenicht, C.; Kam L. C.; Antal, M. J. Jr.; Bian, N.; Cunningham, R. J.; Jones M. Jr. *Ind. Eng. Chem. Res.* **1994**, *33*, 1989.
- Tommila, E.; Kivinen, A. *Suomen Kemistilehti* **1951**, *B24*, 46.
- Hsu, S. U.; Huang, T. T.-S. *Int. J. Chem. Kinet.* **1974**, *5*, 567.
- Kieke, M. L.; Schoppelrei, J. W.; Brill, T. B. *J. Phys. Chem.* **1996**, *100*, 7455.
- Schoppelrei, J. W.; Kieke, M. L.; Wang, X.; Klein, M. T.; Brill, T. B. *J. Phys. Chem.* **1996**, *100*, 14343.
- Maiella, P. G.; Schoppelrei, J. W.; Brill, T. B. *Appl. Spectrosc.* **1999**, *53*, 351.
- Cvetanovic, R. J.; Singleton, D. L. *Int. J. Chem. Kinet.* **1977**, *9*, 481.
- Frisch M. J.; Trucks G. W.; Schlegel H. B.; Scuseria G. E.; Robb M. A.; Cheeseman J. R.; Zakrzewski V. G.; Montgomery J. A. Jr.; Stratmann R. E.; Burant J. C.; Dapprich S.; Millam J. M.; Daniels A. D.; Kudin K.

- N.; Strain M. C.; Farkas O.; Tomasi J.; Barone V.; Cossi M.; Cammi R.; Mennucci B.; Pomelli C.; Adamo C.; Clifford S.; Ochterski J.; Petersson G. A.; Ayala P. Y.; Cui Q.; Morokuma K.; Malick D. K.; Rabuck A. D.; Raghavachari K.; Foresman J. B.; Cioslowski J.; Ortiz J. V.; Stefanov B. B.; Liu G.; Liashenko A.; Piskorz P.; Komaromi I.; Gomperts R.; Martin R. L.; Fox D. J.; Keith T.; Al-Laham M. A.; Peng C. Y.; Nanayakkara A.; Gonzalez C.; Challacombe M.; Gill P. M. W.; Johnson B.; Chen W.; Wong M. W.; Andres J. L.; Gonzalez C.; Head-Gordon M.; Replogle E. S.; Pople J. A. *Gaussian 98*, version A.9; Gaussian, Inc.: Pittsburgh, PA, 1998.
- (30) Becke, A. D. *J. Chem. Phys.* **1993**, *98*, 5648.
- (31) Lee, C.; Yang, W.; Parr, R. G. *Phys. Rev. B* **1988**, *37*, 785.
- (32) Serjeant, E. P.; Dempsey, B. *Ionization Constants of Organic Acids in Aqueous Solutions*; Pergamon: Oxford, 1979.
- (33) Lindsay, W. T. *Proc. Int. Water Conf. Eng. Soc. W. Pa.* **1980**, *41*, 284.
- (34) Uematsu, M.; Franck, E. U. *J. Phys. Chem. Ref. Data* **1980**, *9*, 1291.
- (35) Marshall, W. L.; Franck, E. U. *J. Phys. Chem. Ref. Data* **1981**, *10*, 295.
- (36) Miksa, D.; Li, J.; Brill, T. B. *J. Phys. Chem.*, in press.
- (37) Butler, J. N. *Ion Equilibrium, Solubility and pH Calculation*; John Wiley & Sons: New York, 1998; p 368.
- (38) Li, J.; Brill, T. B. *J. Phys. Chem. A* **2001**, *105*, 6171.
- (39) Gunawardena, N. R.; Brill, T. B. *J. Phys. Chem. A* **2001**, *105*, 1876.
- (40) Crossey, L. J. *Geochim. Cosmochim. Acta* **1991**, *55*, 1515.
- (41) Hall, G. A.; Hanrahan, E. S. *J. Phys. Chem.* **1965**, *69*, 2402.
- (42) Nagy, P. I.; Smith, D. A.; Alagona, G.; Ghio, C. *J. Phys. Chem.* **1994**, *98*, 486.
- (43) Skurski, P.; Simons, J.; Wang X. B.; Wang, L. Sh. *J. Am. Chem. Soc.* **2000**, *122*, 4499.
- (44) Ruelle, P.; Kesselring, U. K.; Nam-Tran, H. *J. Am. Chem. Soc.* **1986**, *108*, 371.
- (45) Ruelle, P. *J. Am. Chem. Soc.* **1987**, *109*, 1722.
- (46) Goddard, J. D.; Yamaguchi, Y.; Schaefer, H. F. *J. Chem. Phys.* **1992**, *96*, 1158.
- (47) Francisco, J. S. *J. Chem. Phys.* **1992**, *96*, 1167.
- (48) Akiya, N.; Savage, P. E. *AIChE J.* **1998**, *44*, 405.
- (49) Ruelle, P. *Chem. Phys.* **1986**, *110*, 263.
- (50) Nguyen, M. T.; Ruelle, P. *Chem. Phys. Lett.* **1987**, *138*, 486.
- (51) Nguyen, M. T.; Sengupta, D.; Raspoet, G.; Vanquickenborne, L. G. *J. Phys. Chem.* **1995**, *99*, 11883.
- (52) Duan X. F.; Page M. *J. Am. Chem. Soc.* **1995**, *117*, 5114.
- (53) Ruelle, P. *J. Comput. Chem.* **1987**, *8*, 158.
- (54) Bock, C. W.; Redington, R. L. *J. Chem. Phys.* **1986**, *85*, 5391.
- (55) Higgins, J.; Zhou, X. F.; Liu, R. F.; Huang, T. T-S. *J. Phys. Chem. A* **1997**, *101*, 2702.
- (56) Tautermann, C. S.; Voegle, A. F.; Loerting, T.; Kohl, I.; Hallbrucker, A.; Mayer, E.; Liedle, K. R. *Chem. Eur. J.* **2002**, *8*, 66.
- (57) Bach, R. D.; Dmitrenko, O.; Glukhovtsev, M. N. *J. Am. Chem. Soc.* **2001**, *123*, 7134.
- (58) McAllister, M. A. *Can. J. Chem.* **1997**, *75*, 1195.
- (59) Chen, J. G.; McAllister, M. A.; Lee, J. K.; Houk, K. N. *J. Org. Chem.* **1998**, *63*, 4611.
- (60) Frey, P. A.; Cleland, W. W. *Bioorg. Chem.* **1998**, *26*, 175.
- (61) Perrin, C. A.; Nielson, J. B. *Annu. Rev. Phys. Chem.* **1997**, *48*, 511.
- (62) Macoas, E. M. S.; Fausto, R.; Lundell, J.; Pettersson, M.; Khriachtchev, L.; Masanen, M. *J. Phys. Chem. A* **2001**, *105*, 3922.
- (63) Price D. J.; Roberts, J. D.; Jorgenson, W. L. *J. Am. Chem. Soc.* **1998**, *120*, 9672.
- (64) Hojendahl, K. *J. Phys. Chem.* **1924**, *28*, 758.
- (65) Rozelle, L. T.; Alberty, R. A. *J. Am. Chem. Soc.* **1957**, *61*, 1637.